Revised version published as: Hongwei Liu, Lei Zhang, Hong Fei Liu, Shuting Chen, Shihua Wang, Zheng Zheng Wong, and Kui Yao*, "High-Frequency Ultrasonic Methods for Determining Corrosion Layer Thickness of Hollow Metallic Components," Ultrasonics, https://doi.org/10.1016/j.ultras.2018.05.006, Vol. 89, pp.166–172, Sept 2018.

# High-Frequency Ultrasonic Methods for Determining Corrosion Layer Thickness of Hollow Metallic Components

Hongwei Liu,[1] Lei Zhang, [1] Hong Fei Liu, [1] Shuting Chen, [1] Shihua Wang,[2] Zheng Zheng Wong, [1] and Kui Yao[1*]

[1] Institute of Materials Research and Engineering, A*STAR, Singapore 138634

[2]National Metrology Center, A*STAR, Singapore 118221

* k-yao@ imre.a-star.edu.sg

**Abstract** Corrosion in internal cavity is one of the most common problems occurs in many hollow metallic components, such as pipes containing corrosive fluids and high temperature turbines in aircraft. It is highly demanded to non-destructively detect the corrosion inside hollow components and determine the corrosion extent from the external side. In this work, we present two high-frequency ultrasonic non-destructive testing (NDT) technologies, including piezoelectric pulse-echo and laser-ultrasonic methods, for detecting corrosion of Ni superalloy from the opposite side. The determination of corrosion layer thickness below ~100 micrometers has been demonstrated by both methods, in comparison with X-CT and SEM. With electron microscopic examination, it is found that with multilayer corrosion structure formed over a prolonged corrosion time, the ultrasonic NDT methods can only reliably reveal outer corrosion layer thickness because of the resulting acoustic contrast among the multiple layers due to their respective different mechanical parameters. A time-frequency signal analysis algorithm is employed to effectively enhance the high frequency ultrasonic signal contrast for the piezoelectric pulse-echo method. Finally, a blind test on a Ni superalloy turbine blade with internal corrosion is conducted with the high frequency piezoelectric pulser-receiver method.

**Keywords** Non-destructive test, Internal Corrosion, Laser-ultrasonic, Piezoelectric pulse-echo, Ultrasonic Wave

## 1. Introduction

Corrosion is one of the most common phenomena occurs in many hollow components, such as pipes containing corrosive fluid or gases and high temperature turbines in aircraft [1-4]. The corrosion inside the hollow components will either form corrosion layers or reduce the wall thickness due to material loss. Early detection of the corrosion inside the hollow components can avoid catastrophic consequences of structural failures. Due to the small dimensions of many hollow components, the internal surfaces are often not accessible. Sometimes the difficulty in determining the extent of the corrosion and the remaining base metal thickness without using destructive inspection lies mainly in that the corrosion is hidden in the hollow component with complex geometry. Non-destructive detecting (NDT) methods, such as dye penetrant testing,

eddy current testing, and thermography can detect defects on the external surface or subsurface. [5-9] Magnetoscope is adopted in engineering practice for the detection of occurrence of internal corrosion, but the accuracy and reliability of such method is not satisfying in industry for determining corrosions hidden in the hollow cavity.[10, 11] Thus, it is often demanded to detect corrosion inside hollow components from the external sides. Compared with the above mentioned NDT methods, ultrasonic testing shows promise for nondestructively measuring the thickness of corrosion and remaining material thickness, because the acoustic properties of corrosion layer are different from the base materials [12-14]. In addition, deep penetration of ultrasonic wave in most of materials makes it suitable for detecting internal corrosion extent and thickness in the hollow components. Therefore, the ultrasonic techniques have been attempted to detect thickness of multilayer structures, corrosion and remaining material thickness [15-22]. However, the resolution of the currently used pulse-echo method is not high enough to detect early-stage corrosion. The utilization of transient Lamb wave can improve the resolution and measure very thin metal sheet thickness, but it can only measure external corrosion layer thickness. In order to yield higher resolution in internal corrosion NDT, here we employ two high-frequency ultrasonic methods, piezoelectric pulse-echo with central frequency of 125 MHz, and broadband laser-ultrasonic, for determining the internal corrosion and remaining base material thickness of Ni superalloy. A time-frequency signal analysis algorithm is applied to further enhance signal contrast and improve the corrosion evaluation reliability. The results are validated by destructive cross-sectional scanning electron microcopy (SEM) and X-ray computed tomography (X-CT). Nowadays, the Ni superalloys are used in many high temperature aerospace components. The corrosion extent will determine if an expensive high temperature Ni-super-alloy component can be kept, repaired or scrapped. Thus, standard Ni-superalloy coupon samples with controlled corrosion extent, which are produced in our dedicatedly designed atmosphere and temperature, are made and measured in both high frequency ultrasonic methods. The interfacial reflection between internal corrosion and remaining base material can be detected and utilized to determine the internal corrosion thickness below ~100 micrometers. We find that multilayer corrosion structures are formed in the Ni superalloy with varied Young's moduli among the different layers when the hot corrosion time is long, and the thicknesses of the corrosion layers determined by the ultrasonic methods correspond to the outer corrosion sublayers, instead of the whole corrosion layers.

Revised version published as: Hongwei Liu, Lei Zhang, Hong Fei Liu, Shuting Chen, Shihua Wang, Zheng Zheng Wong, and Kui Yao*, "High-Frequency Ultrasonic Methods for Determining Corrosion Layer Thickness of Hollow Metallic Components," Ultrasonics, https://doi.org/10.1016/j.ultras.2018.05.006, Vol. 89, pp.166–172, Sept 2018.

## 2. Material and Methods

### 2.1 Specimen Preparation

Ni-superalloy samples with controlled extent of corrosion were prepared, which were tested by the two high frequency ultrasonic methods. The standard Ni-superalloy rods were cut into 2.5 mm-thickness plate by wire cutting, and then the surfaces of the coupons were polished. To form corrosion on coupon surfaces, a tube furnace was employed. Sulfur powder and water vapor were introduced and carried by compressed air at a flow rate of 0.2 NL/min. To simulate the natural corrosion environment, salt agents were spray coated on the surface of the coupons. For the spray coating (at 90 $^{o}$C), $Na_2SO_4$ and $MgSO_4$ with the mole ratio of 47:53 were dissolved in deionized water to form a salt solution with the concentration of 0.02 moles. The hot corrosion process was carried out at 900 $^{o}$C. The overall heating durations were 10, 30, 60, 100, 140, and 180 hours, respectively. The corrosion thicknesses of the Ni superalloy coupon specimens with different corrosion time were examined by SEM. A typical SEM image of the cross section of a Ni-superalloy coupon and the summary of thickness of corrosion layer are presented in Figure 1. In general, the interface between the corrosion layer and the base Ni superalloy is not uniform and the corrosion layer at the coupon edges is found thicker than that of at the center.

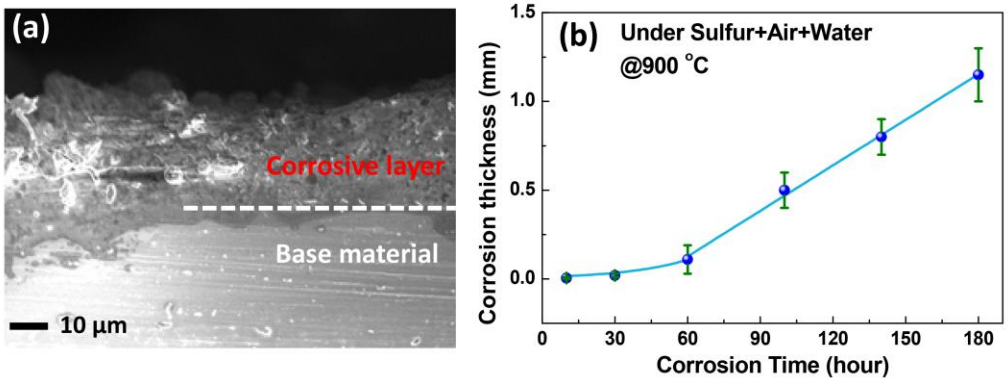


Fig. 1. (a) Cross-sectional SEM image of a Ni-superalloy coupon after hot-corroded at 900 $^{o}$C for 60 hours. (b) Thickness of the corrosion layer of the Ni-superalloy coupons versus the heating duration up to 180 hours.

### 2.2 Piezoelectric Pulse-Echo Test

The schematic of the experimental setup using a high frequency piezoelectric transducer with a central frequency of 125 MHz is shown in Figure 2. The ultrasonic signal travels through the water medium and is reflected by the specimen and received by the transducer. The distance between the transducer and the

Revised version published as: Hongwei Liu, Lei Zhang, Hong Fei Liu, Shuting Chen, Shihua Wang, Zheng Zheng Wong, and Kui Yao*, “High-Frequency Ultrasonic Methods for Determining Corrosion Layer Thickness of Hollow Metallic Components,” Ultrasonics, https://doi.org/10.1016/j.ultras.2018.05.006, Vol. 89, pp.166–172, Sept 2018.

specimen is 1 mm. The transducer is generated and amplified by a dual pulser/receiver model DPR500 from JSR ultrasonic, NY, USA. The received signals are transmitted to a PC digitized card, which has a real-time sampling rate up to 2 GS/s.

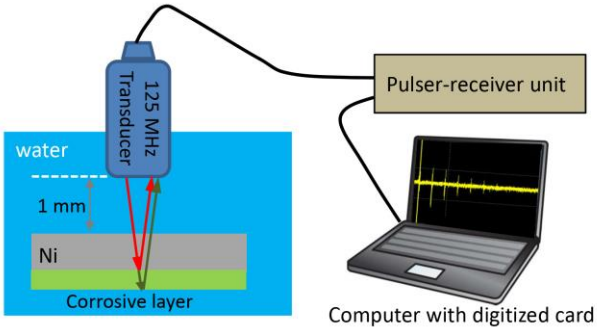


Fig. 2. Experimental setup for piezoelectric pulse-echo test using a 125-MHz piezoelectric transducer.

2.3 Laser-Ultrasonic Test

Experiments using laser-ultrasonic method are conducted and the results are compared with those from the piezoelectric pulse-echo method. In laser-ultrasonic method, reflection mode is utilized to imitate real situation where both generation and detection laser beams are at the front side. Ultrasound is generated by a pulsed Nd:YAG laser (1064 nm, 240 mJ, 4 ns, NL301G, Ekspla, Lithuania), as shown in Figure 3. The ultrasound, after reflection by the back surface of the specimen, caused a small surface motion on the front surface. The reflected ultrasound is detected by a laser ultrasonic receiver, TEMPO, from Bossa Nova Technology, CA, USA. The TEMPO is an interferometer that uses an adaptive reference beam with detection based on the two-wave mixing in a photorefractive crystal. The detector produces a time-varying analog voltage that is proportional to the instaneous displacement at ultrasonic frequencies.

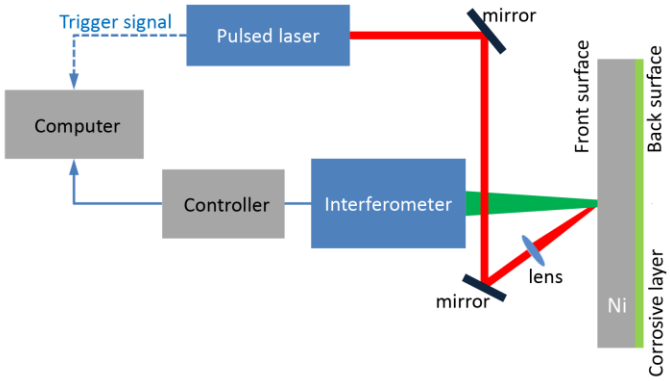


Fig. 3. Experimental setup for laser-ultrasonic measurement.

Revised version published as: Hongwei Liu, Lei Zhang, Hong Fei Liu, Shuting Chen, Shihua Wang, Zheng Zheng Wong, and Kui Yao*, "High-Frequency Ultrasonic Methods for Determining Corrosion Layer Thickness of Hollow Metallic Components," Ultrasonics, https://doi.org/10.1016/j.ultras.2018.05.006, Vol. 89, pp.166–172, Sept 2018.

### 2.4 X-ray Computed Tomography (X-CT)

X-CT (Model: GE Phoenix Nanotom) is conducted on the Ni superalloy coupons as a benchmark. To measure the corrosion layer thicknesses on those samples with different corrosion process times, the parameters of X-CT are adjusted as at 160 kV, 30 μA, 2000 ms Integration time and with optimal setting of sensitivity of the detector in X-CT system. In this case, the minimum gray value can be adjusted properly within the dynamic range of the detector in order to ensure that there is enough X-ray going through the Ni superalloy coupons for obtaining X-CT projection image with optimal contrast.

### 2.5 Nanoindentation Test

Agilent G200 nanoindentation system is used to test the Young's modulus of different layers in Ni superalloy coupons. Stress is applied to a small volume of materials to initiate a deformation. The force and displacement response are recorded simultaneously to obtain the local hardness and the Young's modulus data. Since nanoindentation is a localized measurement, we measured 30 different locations for each layer and took the average as the Young's modulus value of the corrosion layers and base material.

## 3. Results

### 3.1 Piezoelectric Pulse-Echo Results

Typical time-domain longitude signals which are generated and detected with the piezoelectric transducers on Ni superalloy specimens with different corrosion times are presented in Figure 4(a). The first echo indicated by the black line overlapped with the high blue peak is reflected from the interface between Ni superalloy and water, and the second echo indicated by the green line is reflected from the interface between the corrosion layer and water. The first and the second echoes can be located clearly due to their simple wave pattern and high intensity. The thickness of the specimens ($T$), when measured by the piezoelectric pulse-echo ultrasonic method in Figure 2, is a product of the velocity of sound in Ni superalloy and one half the time of flight between the two echoes,

Revised version published as: Hongwei Liu, Lei Zhang, Hong Fei Liu, Shuting Chen, Shihua Wang, Zheng Zheng Wong, and Kui Yao*, "High-Frequency Ultrasonic Methods for Determining Corrosion Layer Thickness of Hollow Metallic Components," Ultrasonics, https://doi.org/10.1016/j.ultras.2018.05.006, Vol. 89, pp.166–172, Sept 2018.

$$T = \frac{vt}{2} \tag{1}$$

where $T$ is the thickness of the specimen, $v$ is the sound velocity of Ni superalloy, and $t$ is the time of flight of two echoes. A typical time-domain signal from a Ni superalloy specimen without corrosion layer is displayed as the reference on the top of Figure 4(a). The thickness of the specimen is 2.13 mm measured by vernier caliper. The two echoes reflect from the two outer surfaces of the specimen, and the transit time between the two echoes is 746 ns. Hence, the sound velocity of the Ni superalloy is 5709 m/s, calculated with Equation (1). The transit time of the two echoes of Ni superalloy specimens with corrosion layers increases with hot-corroded time, as shown in Figure 4(a), which indicates the whole specimen is thicken with corrosion time. The second echoes in Figure 4(a) are enlarged to reveal more details as shown in Figure 4(b). An additional small echo, which may reflect from certain interface inside Ni superalloy specimen, can be distinguished when hot-corroded process is longer than 60 hours. This small echo is hardly observed in time domain signal, however, it clearly shows in frequency domain after a time-frequency analysis is applied. In following sections, the time-frequency analysis will be introduced and the origin of this small echo will be investigated.

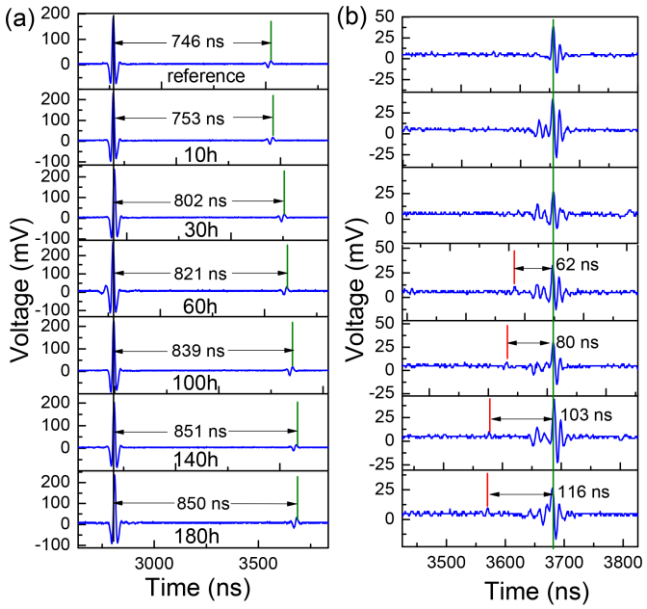


Fig. 4. (a) Typical time domain signals of piezoelectric pulse-echo measurement on Ni superalloy specimens with different thicknesses of corrosion layers. (b) Zoom-in view of the second echo in (a). The signals are offset for comparison of different corrosion layer thickness. The green lines indicate the reflectance from back surface, and the red lines indicate the reflectance from internal interface.

## 3.2 Laser-Ultrasonic Results

Revised version published as: Hongwei Liu, Lei Zhang, Hong Fei Liu, Shuting Chen, Shihua Wang, Zheng Zheng Wong, and Kui Yao*, “High-Frequency Ultrasonic Methods for Determining Corrosion Layer Thickness of Hollow Metallic Components,” Ultrasonics, https://doi.org/10.1016/j.ultras.2018.05.006, Vol. 89, pp.166–172, Sept 2018.

Typical time-domain laser-ultrasonic signals of Ni superalloy specimen with different corrosion layer are presented in Figure 5. There are two reflection peaks, corresponding to reflection from an interface inside Ni superalloy specimen (red arrow) and reflection from back surface, ie. interface between corrosion layer and air (green arrow), respectively. The position of reflection from the back surface suggests the overall thickness of the specimen. It is clearly shown that the whole thickness of the specimens increases with hot-corroded process time, which agrees with piezoelectric pulse-echo result. The reflection from the internal interface with 10-hour and 30-hour hot corrosion process can be clearly distinguished, which indicate laser ultrasonic technology is capable of measuring thin corrosion layer on Ni superalloy specimen. Like piezoelectric pulse-echo results, the origin of the internal reflection will be discussed in following sections.

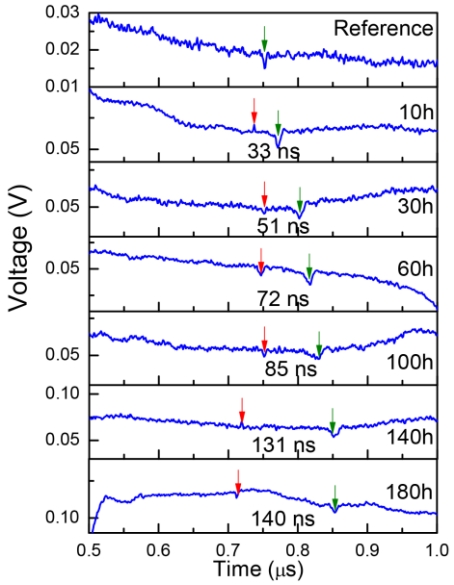


Fig. 5. Reflection signals from internal interface (red arrow) and back surface (green arrow) measured by laser-ultrasonic method.

### 3.3 Origin of the Internal Reflection Investigated by SEM and Nano-Indentation

In order to investigate the origin of the internal reflectance found in both piezoelectric pulse-echo and laser-ultrasonic testing, the Ni superalloy samples were cut and examined by SEM method. Through the detailed SEM examination, the Ni superalloy coupons can be divided into two types based on the duration of hot corrosion: Type I corrosion layer is thin and apparently only contains one single layer, as shown in Figure 6(a). This type includes the coupons after 10, 30 and 60 hour corrosion. Type II corrosion layer is thick with complicated morphology, apparently consisting of at least two sublayers, i.e., outer corrosion layer and inner corrosion layer, as shown in Figure 6(b). The outer corrosion layer is more porous than the inner corrosion

Revised version published as: Hongwei Liu, Lei Zhang, Hong Fei Liu, Shuting Chen, Shihua Wang, Zheng Zheng Wong, and Kui Yao*, "High-Frequency Ultrasonic Methods for Determining Corrosion Layer Thickness of Hollow Metallic Components," Ultrasonics, https://doi.org/10.1016/j.ultras.2018.05.006, Vol. 89, pp.166–172, Sept 2018.

layer. Type II corrosion includes the coupons with 100, 140, and 180 hour hot corrosion. For Type II coupons, as the corrosion comprises multilayer structure and multiple interfaces, it is important to understand at which interface the ultrasonic waves is largely reflected. This will help to analyze the corrosion thickness measurements by ultrasonic methods.

For answering the question above, nanoindentation test was conducted on Ni superalloy coupons. Table 1 gives the measured Young's modulus in each layer of the coupons. It can be seen that the Young's modulus of the outer corrosion sublayer is significantly lower than that of the base material and the inner corrosion layer. In consideration of that the outer corrosion sublayer is much more porous, the acoustic impedance contrast between the outer and inner corrosion layer could be even larger than that of between the inner corrosion layer and the base material. Thus, for sample with thicker corrosion layer, most of ultrasonic signals should be reflected from the interface between the outer and the inner corrosion layers, instead of that between the inner corrosion layer and the base material. In the next section, it can be seen that the thicknesses of corrosion layer obtained by ultrasonic methods correspond well to the outer corrosion sublayer instead of the entire corrosion layer as observed by SEM for the Ni superalloy samples after the prolonged corrosion.

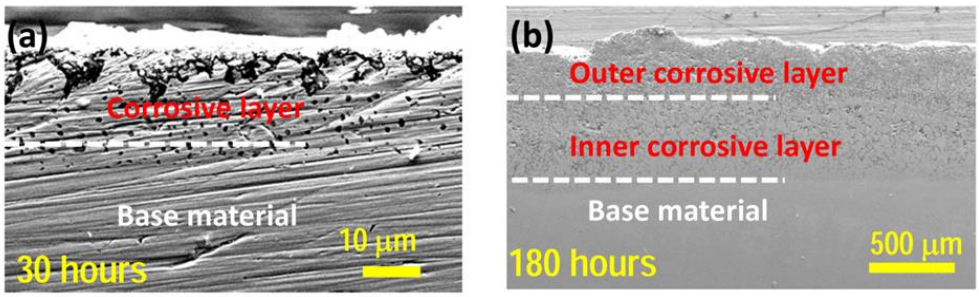


Fig. 6. Cross-sectional SEM images of Ni superalloy coupons after (a) 30-hour and (b) 180-hour corrosion.

Table 1. Young's modulus of the base material and corrosion layers of Ni superalloy coupons

| Corrosion Time of Sample (hours) | Base Materials (GPa) | Corrosion Layer (GPa) | |
|---|---|---|---|
| 10 | 254.0 | 236.0 | |
| 30 | 269.0 | 241.0 | |
| 60 | 248.0 | 159.5 | |
| | | Inner Corrosion Sublayer | Outer Corrosion Sublayer |
| 100 | 240.0 | 189.0 | 62.0 |
| 140 | 239.0 | 158.2 | 46.3 |
| 180 | 256.8 | 149.3 | 57.3 |

Revised version published as: Hongwei Liu, Lei Zhang, Hong Fei Liu, Shuting Chen, Shihua Wang, Zheng Zheng Wong, and Kui Yao*, "High-Frequency Ultrasonic Methods for Determining Corrosion Layer Thickness of Hollow Metallic Components," Ultrasonics, https://doi.org/10.1016/j.ultras.2018.05.006, Vol. 89, pp.166–172, Sept 2018.

### 3.4 Summary of Nickel Superalloy Coupons Results

Table 2 summarizes the thickness of corrosion layers for samples with different hot corrosion times obtained by different methods, i.e., piezoelectric pulser-receiver, laser ultrasonics, X-CT and SEM. The data of the corrosion layer thicknesses determined from the piezoelectric pulser-receiver method in Table 2 are obtained from time-frequency analysis algorithm for enhanced signal-to-noise ratio, with the details of the algorithm explained in the next section. It is evident that the results of the piezoelectric pulse-echo and laser ultrasonic approaches are consistent with each other. The thickness of whole corrosion layer obtained by SEM is much larger than the thickness measured by ultrasonic methods for samples with corrosion time longer than 60 hours. However, if only the thickness of the outer corrosion sublayer is taken into account, the thicknesses of corrosion layers determined by both ultrasonic methods are in good agreement with the outer corrosion sublayer in SEM. This is due to the larger acoustic impedance contrast between the outer and inner corrosion sublayers rather than that of between the inner corrosion sublayer and the base material, as confirmed with the nanoindentation test. The thickness measured by X-CT is consistent with ultrasonic methods for samples with hot corrosion time of up to 140 hours. For the sample with hot corrosion time of 180 hours, X-CT measure the whole corrosion layer thickness, while ultrasonic methods measure the outer corrosion sublayer. X-CT depends on electromagnetic contrast which is different from mechanical contrast and it is also largely affected by parameter setting. It is not a surprise that X-CT shows the results corresponding to the different sublayers in the case of multilayer structures. In our X-CT experimental setting, outer corrosion sublayer thickness is observed for 140-hour corrosion sample while the whole corrosion layer thickness is observed for 180-hour corrosion.

Table 2. Comparison for thickness of corrosion layer measured by different experimental methods [a]

| Corrosion Time (hours) | Piezoelectric pulser-receiver (μm) | Laser-ultrasonics (μm) | X-CT (μm) | SEM (μm) | |
|---|---|---|---|---|---|
| | | | | Whole corrosion layer | Outer corrosion sublayer |
| 10 | 75 | 94 | - | 12 | 12 |
| 30 | 85 | 145 | 132 | 21 | 21 |
| 60 | 191 | 205 | 211 | 108 | 108 |
| 100 | 239 | 242 | 228 | 494 | 207 |
| 140 | 320 | 374 | 391 | 788 | 324 |
| 180 | 334 | 401 | 998 | 1123 | 386 |

[a] It is assumed that sound velocity in corrosion layer is 5709 m/s, which is the same as Ni superalloy.

Revised version published as: Hongwei Liu, Lei Zhang, Hong Fei Liu, Shuting Chen, Shihua Wang, Zheng Zheng Wong, and Kui Yao*, "High-Frequency Ultrasonic Methods for Determining Corrosion Layer Thickness of Hollow Metallic Components," Ultrasonics, https://doi.org/10.1016/j.ultras.2018.05.006, Vol. 89, pp.166–172, Sept 2018.

### 3.5 Time-Frequency Analysis to Improve Signal-to-Noise Ratio of Piezoelectric Pulse-Echo Data

From the ultrasonic testing data in Figure 4(b), it is observed that the ultrasonic echo reflected from the interface between Ni-superalloy base material and corrosion layer is much smaller compared to the back surface echo. It is important to improve the contrast of the ultrasonic signals so that the ultrasonic echo reflected from the corrosion interface can be clearly identified. To achieve this purpose, we transform the time domain ultrasonic signals into time-frequency domain data based on short time Fourier transform. [23-26] As shown in Figure 7, a narrow window (32 ns) of data is first selected and fast Fourier transform (FFT) is performed with the windowed data. After the FFT processing, the frequency spectrum for the windowed data can be obtained. By moving the window continuously at a step of 1 ns in time domain and performing FFT for the windowed data, a time-frequency figure can be generated for the whole time domain. As shown in Figure 8(b), in time-frequency domain, the interface reflection can be more clearly observed than in the time domain in Figure 8(a), and the time of the flight between the interface reflection and back surface reflection can also be determined. Especially for the coupons after 10 and 30 hour hot corrosion, the corrosion layer thicknesses below 100 μm can be clearly identified after time-frequency signal analysis, while they are not able to be observed directly from pulser-receiver raw data. Though there are some differences in the times of flights from the raw data in Figure 8(a) and the FFT processed data in Figure 8(b), the differences of times of flights obtained by the two sets of data range from 0.9% to 8.7%. The difference is considered not significant given the small absolute value of time differences in ns. It can be seen from Figure 8(b) that large noise exists in low frequency range (particularly <50 MHz), which indicates it is not realistic to detect such corrosion layers at low frequency range.

Revised version published as: Hongwei Liu, Lei Zhang, Hong Fei Liu, Shuting Chen, Shihua Wang, Zheng Zheng Wong, and Kui Yao*, “High-Frequency Ultrasonic Methods for Determining Corrosion Layer Thickness of Hollow Metallic Components,” Ultrasonics, https://doi.org/10.1016/j.ultras.2018.05.006, Vol. 89, pp.166–172, Sept 2018.

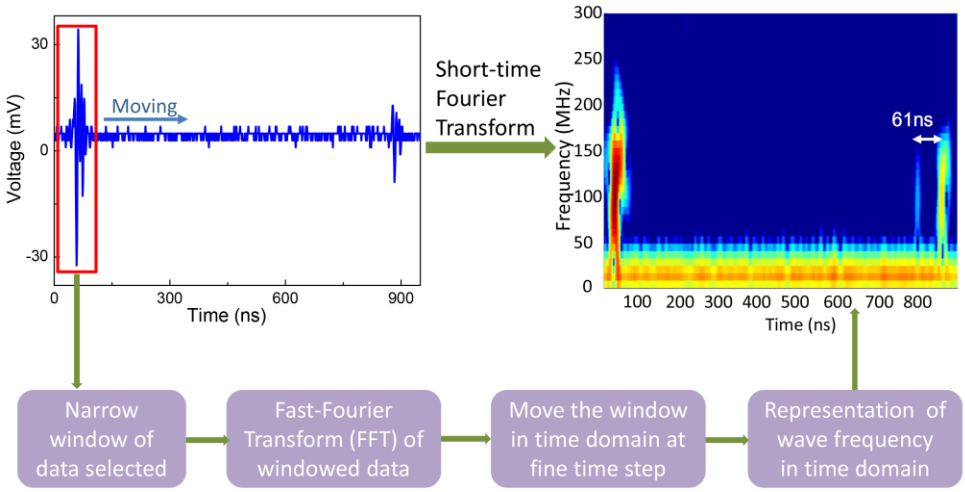


Fig. 7. Illustration of time-frequency algorithm for improving signal contrast of ultrasonic data.

### 3.6 Ultrasonic testing on turbine blade

To further evaluate the feasibility of the high frequency ultrasonic method for determining practical internal corrosion of hollow components, we conducted a blind test on a real high pressure turbine blade with thermal barrier coating. In this blind test, we picked 40 points on the blade for the ultrasonic test point by point. The original ultrasonic signals are subsequently processed by the time-frequency algorithm as explained in the previous section to enhance the signal-to-noise ratio. To conclude the corrosion state from the ultrasonic testing at the 40 points individually, we set 100 μm corrosion thickness as the threshold. For location where corrosion thickness was more than 100 μm, we considered it as “Corroded”, otherwise, it was regarded as “Not Corroded”. After the corrosion state of the 40 points had been determined, the turbine blade was cut by a separate engineer into small slices, and cross-sectional SEM examination was conducted for each of the 40 points without knowing the ultrasonic testing outcome. A comparison is made between the low cost high frequency pulser-receiver ultrasonic NDT method with the expensive destructive point-by-point SEM examinations.

Revised version published as: Hongwei Liu, Lei Zhang, Hong Fei Liu, Shuting Chen, Shihua Wang, Zheng Zheng Wong, and Kui Yao*, "High-Frequency Ultrasonic Methods for Determining Corrosion Layer Thickness of Hollow Metallic Components," Ultrasonics, https://doi.org/10.1016/j.ultras.2018.05.006, Vol. 89, pp.166–172, Sept 2018.

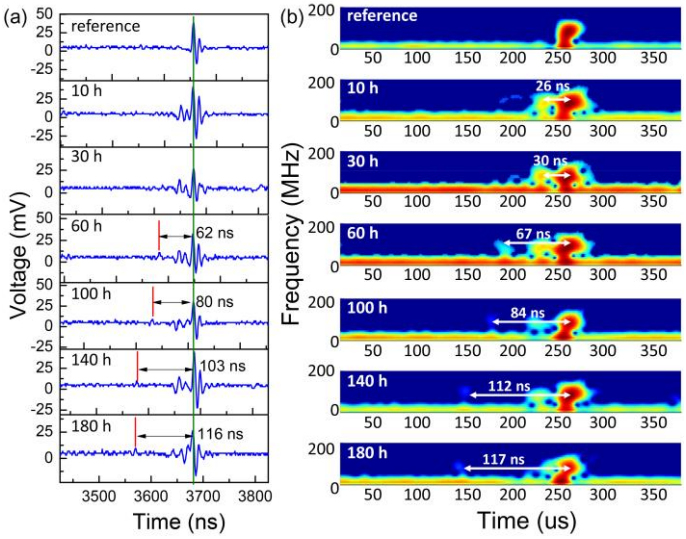


Fig. 8. (a) Raw data of piezoelectric pulse-echo measurement on Ni superalloy coupons. (b) Processed piezoelectric pulse-echo ultrasonic data of Ni superalloy coupons.

Among the 40 points, 15 points were determined as "corroded", and the rest 25 points were determined as "Not corroded" based on the ultrasonic testing results. In contrast, the SEM results showed that 5 points were "corroded" and the rest 35 points were "not corroded". With the validation by the destructive SEM examination, it was found that the ultrasonic method can obtain a true positive rate of 100% and a false negative rate of 0%. This means that the ultrasonic method is acceptable in general for ensuring the safety for evaluating corrosion of turbine blades. However, the ultrasonic method here has a false positive rate of 29%, which may lead to unnecessary repair or scrapping, i.e., extra cost in practical application.

## 4. Discussions

In this work, the internal corrosion layer of Ni superalloy below 100 μm can be well detected with high frequency ultrasonic NDT method. The use of high-frequency ultrasound above 100 MHz through either the pulser-receiver or the laser ultrasonic method makes it feasible to measure the thickness of such a thin corrosion layer. In the literature, this may be the first time to employ such high-frequency ultrasound to quantitatively determine internal corrosion thickness with validated outcome. The progress here will inspire the investigation and application of high frequency ultrasonic NDT method in detection of early-stage corrosion in hollow components.

Revised version published as: Hongwei Liu, Lei Zhang, Hong Fei Liu, Shuting Chen, Shihua Wang, Zheng Zheng Wong, and Kui Yao*, "High-Frequency Ultrasonic Methods for Determining Corrosion Layer Thickness of Hollow Metallic Components," Ultrasonics, https://doi.org/10.1016/j.ultras.2018.05.006, Vol. 89, pp.166–172, Sept 2018.

With a comparison of the results in Figs 4 and 5, laser ultrasonic method exhibits higher detection resolution with the raw data than the pulser-receiver method as its raw data can show the ultrasound reflection for the specimen with shorter corrosion duration. The reason may be the ultrasound signal excited by the sharp laser pulse (4 ns) has even higher frequency components than 125 MHz. However, with the narrowed high frequency ultrasound signal, the piezoelectric pulse-echo method gains comparable resolution below 100 μm (at least up to 75 μm) after the implementation of the time-frequency signal processing algorithm. Compared with laser-ultrasonic method, piezoelectric pulse-echo set-up is portable at much lower cost and without the need for manipulating high-energy laser and sensitive optical system, and thus provides an economical, safe, fast, and user-friendly method for internal corrosion thickness measurements in most of the practical NDT applications. However, in some working conditions, such as high temperature, presence of hazardous gas, or when ultrasonic couplant is not applicable, laser-ultrasonic is an attractive alternative approach attributed to its non-contact feature.

## 5. Conclusions

Two high-frequency ultrasonic NDT methods, piezoelectric pulse-echo and laser-ultrasonic, are demonstrated to be able to determine the thickness of internal corrosion layer of Ni superalloy material, validated by SEM and X-CT. The detection of corrosion layer thickness below ~100 micrometers is realized by both methods. With electron microscopic examination, it is found that with multilayer corrosion structure formed over a prolonged corrosion time, the ultrasonic NDT methods can only reliably reveal outer corrosion sublayer thickness because of the resulting acoustic contrast among the multiple layers due to their respective different mechanical parameters. A time-frequency signal analysis algorithm is applied to further effectively enhance the high frequency ultrasonic signal contrast for the piezoelectric pulse-echo method. Finally, a blind test on a Ni superalloy turbine blade with internal corrosion is conducted with the high frequency piezoelectric pulser-receiver method. Compared with destructive cross-sectional SEM examination, a true positive rate of 100% and a false negative rate of 0% indicate that the high frequency ultrasonic method is acceptable for ensuring the safety for evaluating corrosion of turbine blades, although a false positive rate of 29% may lead to unnecessary repair or scrapping.

Revised version published as: Hongwei Liu, Lei Zhang, Hong Fei Liu, Shuting Chen, Shihua Wang, Zheng Zheng Wong, and Kui Yao*, “High-Frequency Ultrasonic Methods for Determining Corrosion Layer Thickness of Hollow Metallic Components,” Ultrasonics, https://doi.org/10.1016/j.ultras.2018.05.006, Vol. 89, pp.166–172, Sept 2018.

**Acknowledgement**

This work was supported by the Aerospace Program of A*STAR, Singapore through the project IMRE/14–2P1114, and A*STAR Science and Engineering Research Council (SERC) Grant number 1421500068.

## Reference

[1] N. Eliaz, G. Shemesh, R.M. Latanision, Hot corrosion in gas turbine components, Engineering Failure Analysis, 9 (2002) 31-43.
[2] S. Nešić, Key issues related to modelling of internal corrosion of oil and gas pipelines – A review, Corros. Sci., 49 (2007) 4308-4338.
[3] Q. Feng, R. Li, B. Nie, S. Liu, L. Zhao, H. Zhang, Literature Review: Theory and Application of In-Line Inspection Technologies for Oil and Gas Pipeline Girth Weld Defection, Sensors, 17 (2017) 50.
[4] S. Mustapha, A. Braytee, L. Ye, Multisource Data Fusion for Classification of Surface Cracks in Steel Pipes, Journal of Nondestructive Evaluation, Diagnostics and Prognostics of Engineering Systems, 1 (2018) 021007-021007-021011.
[5] R.D. Adams, P. Cawley, A review of defect types and nondestructive testing techniques for composites and bonded joints, NDT International, 21 (1988) 208-222.
[6] X. Li, B. Gao, W.L. Woo, G.Y. Tian, X. Qiu, L. Gu, Quantitative Surface Crack Evaluation Based on Eddy Current Pulsed Thermography, IEEE Sens. J., 17 (2017) 412-421.
[7] Y. He, M. Pan, F. Luo, G. Tian, Pulsed eddy current imaging and frequency spectrum analysis for hidden defect nondestructive testing and evaluation, NDT & E International, 44 (2011) 344-352.
[8] J. Liu, J. Gong, L. Qin, Y. Wang, Study on Lock-in Thermography Defect Detectability for Carbon-Fiber-Reinforced Polymer (CFRP) Sheet with Subsurface Defects, Int. J. Thermophys., 36 (2015) 1259-1265.
[9] C. Xu, J. Xie, W. Huang, G. Chen, X. Gong, Improving defect visibility in square pulse thermography of metallic components using correlation analysis, MSSP, 103 (2018) 162-173.
[10] A.Y. Krasovskii, V.A. Vainshtok, Use of fracture mechanics to evaluate the bearing capacity and remaining life of rotors in turbomachinery, Strength of Materials, 14 (1982) 997-1005.
[11] H. Kwun, A.E. Holt, Feasibility of under-lagging corrosion detection in steel pipe using the magnetostrictive sensor technique, NDT & E International, 28 (1995) 211-214.
[12] G. Sposito, C. Ward, P. Cawley, P.B. Nagy, C. Scruby, A review of non-destructive techniques for the detection of creep damage in power plant steels, NDT & E International, 43 (2010) 555-567.
[13] K. Reber, M. Beller, H. Willems, O.A. Barbian, A new generation of ultrasonic in-line inspection tools for detecting, sizing and locating metal loss and cracks in transmission pipelines, in: Ultrasonics Symposium, 2002. Proceedings. 2002 IEEE, 2002, pp. 665-671.
[14] A. Demma, P. Cawley, M. Lowe, A.G. Roosenbrand, B. Pavlakovic, The reflection of guided waves from notches in pipes: a guide for interpreting corrosion measurements, NDT & E International, 37 (2004) 167-180.
[15] R.G. Maev, H. Shao, E.Y. Maeva, Thickness Measurement of a Curved Multilayered Polymer System by Using an Ultrasonic Pulse-Echo Method, Mater. Charact., 41 (1998) 97-105.
[16] R. Raišutis, R. Kažys, L. Mažeika, Application of the ultrasonic pulse-echo technique for quality control of the multi-layered plastic materials, NDT & E International, 41 (2008) 300-311.
[17] R.J. Dewhurst, C. Edwards, A.D.W. McKie, S.B. Palmer, Estimation of the thickness of thin metal sheet using laser generated ultrasound, Appl. Phys. Lett., 51 (1987) 1066-1068.
[18] M. Kobayashi, C.K. Jen, J.F. Bussiere, K.T. Wu, High-temperature integrated and flexible ultrasonic transducers for nondestructive testing, NDT & E International, 42 (2009) 157-161.
[19] G. Waag, L. Hoff, P. Norli, Air-coupled ultrasonic through-transmission thickness measurements of steel plates, Ultra, 56 (2015) 332-339.
[20] W. Gao, C. Glorieux, J. Thoen, Laser ultrasonic study of Lamb waves: determination of the thickness and velocities of a thin plate, IJES, 41 (2003) 219-228.
[21] L.P. Scudder, D.A. Hutchins, G. Ningqun, Laser-generated ultrasonic guided waves in fiber-reinforced plates-theory and experiment, IEEE Transactions on Ultrasonics, Ferroelectrics, and Frequency Control, 43 (1996) 870-880.
[22] S. Mustapha, Y. Lu, J. Li, L. Ye, Damage detection in rebar-reinforced concrete beams based on time reversal of guided waves, Structural Health Monitoring, 13 (2014) 347-358.
[23] G. Andria, F. Attivissimo, N. Giaquinto, Digital signal processing techniques for accurate ultrasonic sensor measurement, Measurement, 30 (2001) 105-114.
[24] M. Fink, F. Hottier, J.F. Cardoso, Ultrasonic signal processing for in vivo attenuation measurement: Short time Fourier analysis, UltIm, 5 (1983) 117-135.
[25] A. Benammar, R. Drai, A. Guessoum, Ultrasonic flaw detection using threshold modified S-transform, Ultra, 54 (2014) 676-683.
[26] L. Cohen, Time-frequency Analysis, Prentice Hall PTR, 1995.